Journal of Plant Growth Regulation (2021) 40:1881–1893
https://doi.org/10.1007/s00344-020-10237-7

# Co-regulation of Auxin and Cytokinin in Anthocyanin Accumulation During Natural Development of Purple Wheat Grains

**Luhua Li[1,2] · Guiping Yang[1,2] · Mingjian Ren[1,2] · Zhongni Wang[3] · Yashu Peng[1,2] · Ruhong Xu[1,2]**

Received: 20 May 2020 / Accepted: 24 September 2020 / Published online: 6 October 2020


## Abstract

Purple-colored wheat is a kind of wheat with purple-colored grains that contain significant levels of anthocyanins, and anthocyanins benefit human health because of their antioxidant activities. Many studies indicated stresses can significantly induce anthocyanin accumulation during grain development. However, the effects of auxins and cytokinins (CKs) on anthocyanin accumulation during purple grain development have been poorly investigated. Here, we explored the relationships of endogenous auxins and CKs with anthocyanin accumulation during the natural development of purple wheat grains. We found dynamic change of auxin content was consistent with anthocyanin accumulation trend during seed development, which began to rapidly increase from 25 dpa up to the maximum level at 35 dpa. Conversely, CKs, including iPR, cZ, czR, tZ, and tZR, significantly decreased at 25 dpa. The relative expression of Gz*PIN1*, Gz*LAX3*, Gz*IAA12*, Gz*ABP1*, Gz*ZOG2*, Gz*UGT* , and Gz*CKX2* was assessed, which is in agreement with ABA and CK accumulation. The findings indicated that auxins and CKs were involved in anthocyanin accumulation during purple grain development in an antagonistic manner. Meanwhile, the contents of the antioxidant enzymes POD and CAT were consistent with the dynamic change in the anthocyanin accumulation rate, which implied that ROS signaling participates in the regulation of anthocyanin accumulation.

**Keywords** Purple wheat · Anthocyanin · Auxin · Cytokinins

## Abbreviations

| | |
|---|---|
| PIN | PIN-FORMED |
| LAX | LIKE AUXIN1 |
| IAA | Indole-3-acetic acid |
| ABP | Auxin-binding protein |
| ZOG | CK-O-glucosyltransferases |
| UGT | Uridine diphosphate glycosyltransferases |
| CKX | CK oxidases |
| POD | Peroxidase |
| CAT | Catalase |
| 2,4-D | 2,4-Dichlorophenoxyacetic acid |
| NAA | Naphthalene acetic acid |
| ARF | Auxin response factor |
| SOD | Superoxide dismutase |
| TAA | Tryptophan aminotransferase of *Arabidopsis* |
| TAR | Tryptophan aminotransferases |
| YUC | YUCCA |
| AKR | Aldo-ketoreductase |
| 5GN4 | Auxin-induced protein 5NG4 |
| ARP | Auxin-repressed protein |
| AHKs | *Arabidopsis* Histidine kinases |
| ZNG | CK-N-glucosyltransferase |
| AUX/IAA | AUXIN/indole acetic acid |

Luhua Li and Guiping Yang have contributed equally to this work.

✉ Ruhong Xu
xrhgz@163.com

[1] College of Agriculture, Guizhou University, Guiyang 550025, China

[2] Guizhou Sub-Center of National Wheat Improvement Center, Guiyang 550025, China

[3] Guizhou Rice Research Institute, Guizhou Provincial Academy of Agricultural Science, Guiyang 550006, China

## Introduction

Wheat (*Triticum aestivum* L.) is an important crop worldwide. Purple-colored wheat has purple-colored grains that contain significant levels of anthocyanins, commonly in the pericarp (Zeven 1991; Liu et al. 2010). The anthocyanins have antioxidant activities, which benefit human health, including reducing the incidence of colon cancer, protecting blood vessels and having anti-inflammatory effects (Hirawan et al. 2011; Zilić et al. 2012; Cavalcanti et al. 2011). The

correlation results between antioxidant activity and contents of bioactive phytochemicals in purple grains have shown a high correlation for cyanidin and pelargonidin. It is shown anthocyanins content changes depending on growth stage (Sytar et al. 2018). Therefore, the breeding of purple-colored wheat, and its nutritional value, have attracted attention (Bartl et al. 2015).

Anthocyanins, which are widely found in higher plants, such as vegetables, fruits, and cereal grains, are water-soluble pigments belonging to the flavonoid group (Chen et al. 2013). The anthocyanin content increases significantly in response to stresses (e.g., drought) (Ma et al. 2014) and phytohormones (Olivares et al. 2017). Both auxins, such as IAA, 2,4-D and NAA, and CKs regulate anthocyanin metabolism (Murthy et al. 2014; Zhou et al. 2008; Das et al. 2012). For auxins, certain IAA levels inhibit IAA signaling, resulting in the decreased expression of anthocyanin-related genes, which then leads to the suppression of anthocyanin biosynthesis in strawberry (*Fragaria ananassa* L.), radish (*Raphanus sativus* L.), grape (*Vitis vinifera* L.) and *Arabidopsis thaliana* (Guo et al. 2018; Chen et al. 2016; Jia et al. 2017; Shi and Xie 2011; Liu et al. 2014). Additionally, ARF7 and ARF19 mutants have overaccumulations of anthocyanins in *Arabidopsis* shoots (Huang et al. 2018). However, Park et al. reported recently that appropriate auxin concentrations increase anthocyanin accumulation through enhanced production of cyanidin 3-*O*-glucoside and cyanidin 3-*O*-rutinoside in Tartary buckwheat (Park et al. 2016). In addition, anthocyanins are regulators of polar auxin carriers, suggesting crosstalk between auxin- and anthocyanin-dependent processes (Lazar and Goodman 2006; Brown and Aaron 2001; Buer and Muday 2004). CKs treatments stimulate anthocyanin accumulation through the up-regulation of anthocyanin biosynthesis genes, which then affect the transcript levels of *MYB*-related regulatory genes in *Arabidopsis* (Hammer 1995; Das et al. 2012; Nguyen et al. 2015) and maize (Piazza et al. 2002). Ji et al. reported that certain CK levels promote anthocyanin accumulation, and if the CK level exceeds a certain concentration, then the anthocyanin accumulation decreases in apple calli (Ji et al. 2015). Exogenous CKs also enhance anthocyanin accumulation through activation of anthocyanin biosynthesis genes through type-B response regulatory genes in pear (Jun et al. 2017). Thus, the inhibitory effects of exogenous auxin on anthocyanin biosynthesis can be influenced by CKs, while co-treatments with auxins plus CKs at certain concentrations significantly enhance CK-induced increases of anthocyanin in apple calli (Ji et al. 2015). However, less is known about the interactions of auxins and CKs during wheat grain development.

In this study, we investigated the effects of variations in endogenous auxin and CK levels on anthocyanin accumulation during the natural development of purple wheat grains. Based on the transcriptome sequencing results, dynamic expression levels of eight auxin-related and seven CK-related genes during anthocyanin accumulation at different developmental periods of purple wheat grains were determined. Furthermore, the endogenous contents of auxins and CKs were detected. Our results demonstrated that endogenous auxins and CKs have antagonistic roles during anthocyanin accumulation in purple wheat grains.

## Materials and Methods

### Plant Materials and Sample Preparation

*Triticum aestivum* L. cv. Guizi 1 (GZ1, Certificate No. Qian 2015003) (Li et al. 2018), which was stored in the Guizhou Sub-Center of National Wheat Improvement Center at the College of Agriculture in Guizhou University, showed strong advantages in yield, quality and disease resistant. GZ1 was planted on the experimental farm in accordance with Li et al. (2018) and the field management (including watering, weeding and fertilization) was carried out in a unified manner.

The grain samples were prepared in accordance with Li et al. (2018). The developing caryopses were selected from spikes at identical flowering stages at 10-, 25- and 35-days post anthesis (dpa), and samples were stored in − 80 °C. The caryopses from three spikes of different plants were selected and used as repeats for RNA extraction, anthocyanin determination, phytohormone determination and enzyme activity determination.

### RNA Isolation and Quantitative Real-Time PCR

Total RNA from wheat grains was extracted using an EASYspin Plus Complex Plant RNA Kit (Aidlab, Beijing, China), and then the first-strand cDNA was synthesized from 1 μg of RNA using a TRUEscript 1st Strand cDNA Synthesis Kit with gDNA Eraser (Aidlab, Beijing, China). The β-actin gene was used as the internal control, and the qRT-PCR analysis was performed using LightCycler480 SYBR Green (Bio-Rad, CFX 96 Touch, USA). And then, the Delta Delta CT relative quantitation ($2^{-\Delta\Delta ct}$) was used to calculate the relative expression (Livak and Schmittgen 2001). The primers for qRT-PCR are listed in Table 1.

### Extraction and Measurement of Total Anthocyanin

The extraction and quantitative determination of anthocyanin levels were performed in manners similar to those of Li et al. (2018). The frozen samples were weighed (0.5 g) and ground into a powder in liquid nitrogen, and then 4 mL acidified ethanol was added and mixed with the sample for anthocyanin extraction. Total anthocyanin was determined by measuring the absorbance at 527

**Table 1** Sequences of specific genes for the qRT-PCR analysis

| Gene name | Primer sequence (5′–3′) |
|---|---|
| Gz*PIN1*-7D_F | GACGGCAGGAGGGACAT |
| Gz*PIN1*-7D_R | CGGCGTTGGTGAGGTTG |
| Gz*LAX3*-1D_F | ACCGCCTACCTCATCAGCA |
| Gz*LAX3*-1D_R | ACCCCTGCCCTTGTAACTC |
| Gz*IAA12*-5A_F | AGGCCATGTTCGTCTGCTT |
| Gz*IAA12*-5A_R | GCCGTCCTTGTCCTCGTAG |
| Gz*ARF13*-7D_F | TCTACCCAAGGACGAGGTG |
| Gz*ARF13*-7D_R | CAGGTGTTGAGGATGTGGAG |
| Gz*ARF17*-7A-T1_F | TCCTTCTCGTCCTCAGTCC |
| Gz*ARF17*-7A-T1_R | ATCCACCAAGCAACCTCTT |
| Gz*ABP1*-5D_F | CATCGTCGCCTCCTACCTC |
| Gz*ABP1*-5D_R | GTCCCGTGGTTGTGCTTCT |
| Gz*AKR1*-7B2_F | TCAAGGGGATGATGTTGTTC |
| Gz*AKR1*-7B2_R | TCTTCACGTATCTGGCTGCT |
| Gz*5NG4*-7A1_F | GAGTCACGGTCTTCGCTTG |
| Gz*5NG4*-7A1_R | TTATTCTGGGGATGTTGCCT |
| *Actin*-F | CCAAGGCGGAGTACGATGAGTCT |
| *Actin*-R | TTCATACAGCAGGCAAGCACCAT |
| Gz*ZOG2*-2D_F | TGAGGACCAAGTGAAGAACG |
| Gz*ZOG2*-2D_R | CAGCAGGAAGTTGAACAGGA |
| Gz*ZOG2*-7D_F | GGTGTTCCTCACGCACTCT |
| Gz*ZOG2*-7D_R | TCATCCCCAATCTCCATACC |
| Gz*ZOG3*-7A_F | AGGTGGTGGAAGGTTTCATT |
| Gz*ZOG3*-7A_R | CATTGGGAACGCCAGTATT |
| Gz*UGT*-3D1_F | ACCCATAACGGCTGGAACT |
| Gz*UGT*-3D1_R | TTGCCCTCTAACTCAAACCC |
| Gz*AHK3*-3D-T1_F | GCTTATGTGATTGCTTTGCTC |
| Gz*AHK3*-3D-T1_R | TGTAGCCAGGAACTGTGACTT |
| Gz*CKX1*-2D_F | CAGTTCTTGGTGGGCTTGG |
| Gz*CKX1*-2D_R | GCTCTTGGTCCTTGGTGAATG |
| Gz*CKX2*-3A_F | ACCGACTACCTTCACCTCACC |
| Gz*CKX2*-3A_R | GTCCCCGTGCTTTTCCTTT |
| Gz*CKX2.4*-3D3_F | GTCGTCATCGTCCTTCTGCT |
| Gz*CKX2.4*-3D3_R | GCGTCTCCAGCCTCTTTTC |
| Gz*MYB*-7D1_F | GCCGAACAGACAACGAAATC |
| Gz*MYB*-7D1_R | GCAGGGACGGAGGTAGACA |
| Gz*MYC*-2A1_F | ATTGATGGGTGGTGTGCTT |
| Gz*MYC*-2A1_R | TCGTCTACTGATGGGATGGA |
| Gz*CHS*-F | GCTCATCTCCAAGAACATC |
| Gz*CHS*-R | CGTATTCGGAGAGGACAT |
| Gz*ANS*-F | GATCAACAGGAGGAGGAG |
| Gz*ANS*-R | CCTTCTTCACCACCTTGT |

with Evolution 220 (Thermo Fisher, USA) and calculated using the following formula: anthocyanin content (mg/Kg) = (C × V)/m, where C represents the anthocyanin concentration, V represents the volume , and m represents the sample weight.

## The Differentially Expression of Auxin- and CK-Pathway Genes in the Anthocyanin Biosynthesis Pathway

The differentially expressed genes of auxin- and CK-pathway genes in 10 dpa, 25 dpa, and 35 dpa were filtered from the KEGG biological pathway annotation. The number of clusters was set to 30. Venn diagrams were generated using the online tool at https://www.bioinformatics.psb.ugent.be/webtools/Venn/. The expression levels of these genes were calculated using FPKM value (fragments per kb per million reads), and the value of $\log2^{Ratio}$ (the ratio was from the FPKM values of 25 dpa VS 10 dpa, 35 dpa VS 10 dpa, and 35 dpa VS 25 dpa) was used to draw the heat map of gene expression (Excel 2013, USA). Furthermore, real-time PCR was performed to verify the accuracy of genes expression including auxin-pathway genes (Gz*PIN1*, Gz*LAX3*, Gz*IAA12*, Gz*ARF13*, Gz*ARF17*, Gz*ABP1*, Gz*AKR1*, and Gz*5NG4*) and CK-pathway genes (Gz*ZOG2*, Gz*ZOG3*, Gz*UGT*, Gz*AHK3*, Gz*CKX1*, Gz*CKX2*, and Gz*CKX2.4*). The experiment was performed with ≥ 3 replicates to calculate the average value. Statistical significance was determined using Student's *t*-test.

## Determination of Antioxidant Enzymes

The extraction and determination of the antioxidant enzymes POD, CAT, and SOD were performed in accordance with the instructions in the Cominbio kit (Jiangsu, China). The frozen samples (0.1 g) were ground into powders in liquid nitrogen, and then 1 mL extraction solution was added. The mixture was homogenized on ice in an EP tube. Then, the tube was centrifuged at 8000×*g* for 10 min in 4 °C, and the supernatant was used for activity detection with a Multiskan FC Microplate reader (Thermo Fisher, USA). For the SOD content, 200 µL of the supernatant was placed in an ELISA plate and incubated for 30 min at room temperature. Then, the absorbance (A) was measured at 560 nm, and the sample and reagent blank were recorded as A1 and A0, respectively. The inhibition percentage (IP) was calculated using the following formula: IP = (A0–A1)/A0 × 100%. The SOD content was calculated using the following formula: SOD content $(U/g) = 11.11 \times IP \times (1–IP)^{-1} \times m^{-1}$, where m represents the sample weight. For the POD content, 200 µL of the supernatant was placed in an ELISA plate, and the POD content was measured at 1 min and 2 min at 470 nm and recorded as B1 and B2, respectively. Then, the following formula was applied: POD content $(U/g) = 4000 \times (B2-B1) \times m^{-1}$, where m represents the sample weight. For the CAT content, 200 µL of the supernatant was placed in an ELISA

plate, and the CAT content was measured at 0 min and 1 min at 240 nm and recorded as C1 and C2, respectively. Then, the following formula was applied: CAT content (U/g) = 918 × (C2–C1) × $m^{-1}$, where m represents the sample weight.

### Determination of Phytohormones

The extraction and determination of phytohormone levels were performed in accordance with Shao et al. (2019). The frozen samples (80 mg) were ground to a powder in liquid nitrogen. The powder was added to 1 mL ethyl acetate (containing 50 µL internal standards) and shaken for 2 min to mix well. Then, phytohormones were extracted from the powder at 4 °C for 12 h in the dark. The supernatant (800 µL) was collected after centrifugation (14,000×*g* for 10 min at 4 °C) and was then evaporated to dryness under N2. The residue was resuspended in 100 µL 50% acetonitrile (v/v). After being centrifuged (14,000×*g* for 10 min at 4 °C), the supernatant was then analyzed by HPLC–ESI–MS/MS at the Shanghai Applied Protein Technology Company (Shanghai, China). The following steps were the same as described Shao et al. (2019).

## Results

### The Phenotype and Anthocyanin Accumulation During the Natural Development of GZ1 Grains

Natural grain development was observed and the change in caryopsis size was calculated. The width increased 1.4-fold and the length increased 1.71-fold from 5 to 20 dpa, respectively. Then, the increment rate of grain size being decreased gradually until it reached its final size (Fig. 1b). Visible effects of anthocyanin accumulation appeared at 20 dpa and then gradually spread to almost all of the grain surface (Fig. 1a). Subsequently, the anthocyanin content began to rapidly increase at 20 dpa and reached a maximum level by 35 dpa, which was consistent with phenotypic observations (Fig. 1c).

### Dynamic Expression of Auxin- and CK-Pathway Genes During Anthocyanin Biosynthesis at Different Grain Development Periods

Based on the transcriptome sequencing results of three important periods (10, 25, and 35 dpa) for anthocyanin biosynthesis, the upregulated expression of structural and regulatory genes may result in anthocyanin biosynthesis and the resulting coloration of GZ1 grains (Li et al. 2018). In order to identify transcripts common at different grain developmental periods, Venn diagrams of auxin-pathway genes (Fig. 2a–c) and cytokinin-pathway genes (Fig. 2d–f) were generated separately for the upregulated and for the downregulated transcripts at 10, 25 and 35 dpa. For the auxin-pathway genes, the highest overlap was the upregulated transcripts. For the cytokinin -pathway genes, the highest overlap was the downregulated transcripts.

Then, we studied dynamic changes in the expression of auxin- and CK-related genes during anthocyanin biosynthesis at different grain development periods in GZ1 grains. Herein, 22 auxin-related genes that underwent significant expression changes were selected from transcriptome sequencing results (Li et al. 2018). The expression of the auxin efflux transporter gene Gz*PIN1* and auxin influx transporter gene Gz*LAX3* was significantly higher at 25 dpa and 35 dpa than at 10 dpa, and exhibited dynamic increased from 10 to 25 dpa and then decreased from 25 to 35 dpa. However, the expression level of the auxin influx transporter gene

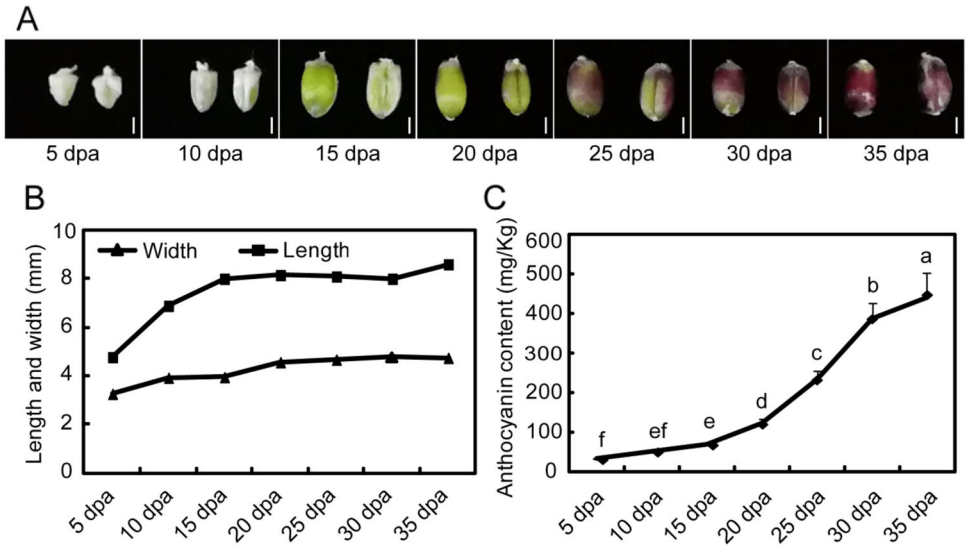


**Fig. 1** Phenotypic observations and anthocyanidin content determinations during the natural development of GZ1 grains. **a** The phenotypic observation at 5, 10, 15, 20, 25, 30, and 35 dpa. **b** Dynamic changes in grain size during natural grain development. **c** Dynamic changes in anthocyanidin content during natural grain development

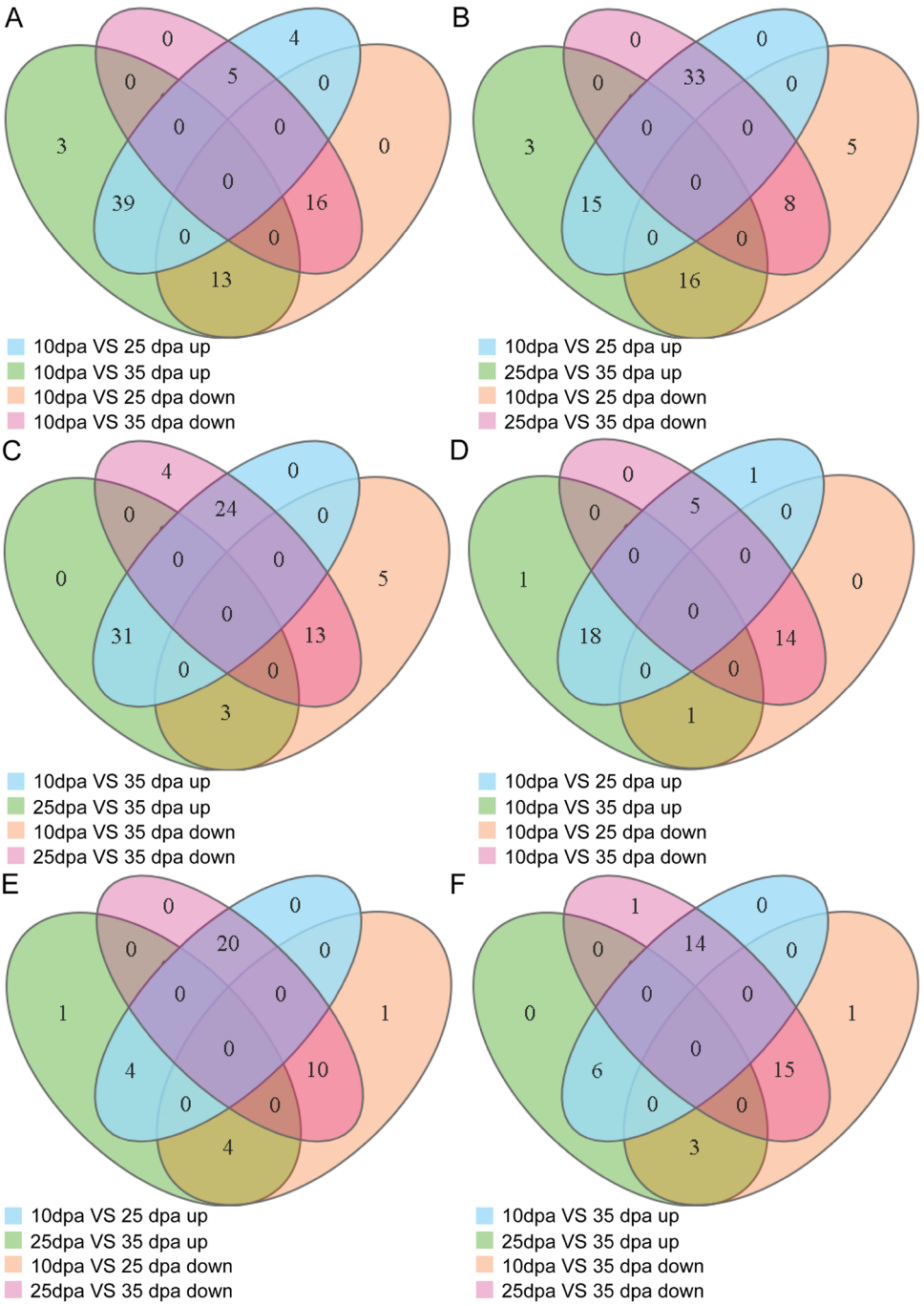


**Fig. 2** Venn diagram analysis of downregulated and upregulated transcripts at different grain development stages 10dpa, 20dpa, and 35dpa. **a–c** Venn diagram analysis of auxin-pathway genes. **d–f** Venn diagram analysis of cytokinin-pathway genes

Gz*LAX2* gradually decreased during anthocyanin accumulation. Here, nine *AUX/IAA* genes and six *ARF* genes related to auxin signaling were selected. The expression levels of Gz*IAA1*, *-3*, *-4*, *-12*, Gz*IAA14–16*, and Gz*IAA30* were significantly higher at 25 dpa and 35 dpa than at 10 dpa, and Gz*IAA1*, *-3*, *-15*, *-16* and *-30* exhibited dynamic increased from 10 to 25 dpa and then decreased from 25 to 35 dpa. However, Gz*IAA4*, *-12* and *-14* gradually increased. Additionally, the expression of Gz*IAA19* decreased from 10 to 25 dpa and then increased from 25 to 35 dpa. The six *ARF* genes showed transcriptomic diversity and complexity during grain development, among which Gz*ARF4*, *-5* and *-17* decreased from 10 to 25 dpa and then increased from 25 to 35 dpa in contrast to Gz*ARF8*. Gz*ARF6* gradually increased and Gz*ARF13* gradually decreased during grain development. Overall, our data indicated that *AUX/IAA* genes may positively correlated with anthocyanin accumulation during the natural development of GZ1 grains, while *ARF* genes may play negative roles. The auxin-binding protein gene (Gz*ABP1*) and auxin-induced protein genes (Gz*AKR1*,

Gz*5GN4*, and Gz*ARP*) also showed transcriptomic diversity and complexity during grain development. GZ1 is a polyploid wheat, and a heat map of these genes, including copies and alternatively spliced transcripts, was constructed (Fig. 3).

In total, 10 significantly changed CK-related genes, including CK-O-glucosyltransferases (*ZOG*s), uridine diphosphate glycosyltransferases (*UGT*s), *Arabidopsis* histidine kinases (*AHK*s), CK-N-glucosyltransferase (*ZNG*s), and CK oxidases (*CKX*s), were selected for heat map construction (Fig. 4). The expression levels of Gz*ZOG2*, Gz*ZOG3* and Gz*ZNG2* were significantly higher at 25 dpa and 35 dpa than at 10 dpa, it increased from 10 to 25 dpa and then decreased from 25 to 35 dpa. The *UGT* on chromosome 3 gradually decreased during grain development in contrast to the gene on chromosome 6A. The CK receptor Gz*AHK3* decreased from 10 to 25 dpa and then increased from 25 to 35 dpa. The five Gz*CKX* genes showed transcriptomic diversity and complexity during grain development, with Gz*CKX1*-NEW, Gz*CKX2.4*-3A, Gz*CKX2.4*-3B1, Gz*CKX2.4*-3D1, Gz*CKX2.4*-3D3, Gz*CKX2*-3A, and Gz*CKX3*-7A gradually decreased; Gz*CKX1*-2D, Gz*CKX2.4*-3B2, Gz*CKX2.4*-3D2, Gz*CKX3*-7B, Gz*CKX3*-U1, Gz*CKX8*-2A, and Gz*CKX8*-2B increased from 10 to 25 dpa and then

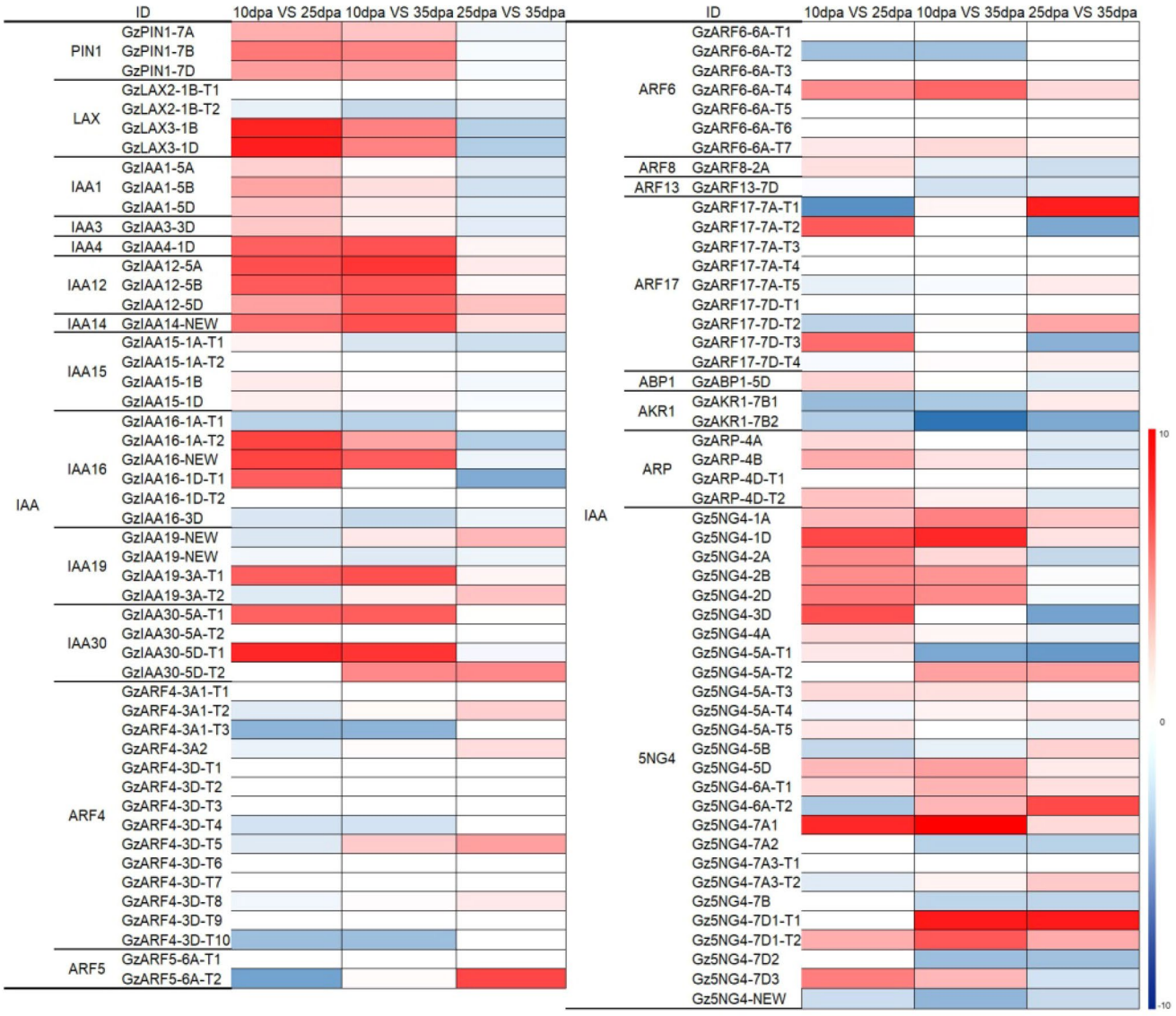


**Fig. 3** Heat map of auxin-pathway genes, including copies and alternatively spliced transcripts, during anthocyanin accumulation in GZ1 grains. Different combinations of numbers and letters (7A, 7B, 7D, 1B, 1D etc.) represent different chromosomal locations. "New" indicates that the chromosomal location is presently not clear. The same chromosome with different numbers represents corresponding copies of a gene located on that chromosome. Numbers after a capital "T" (T1, T2, T3, etc.) represent alternatively spliced transcripts of corresponding genes or copies

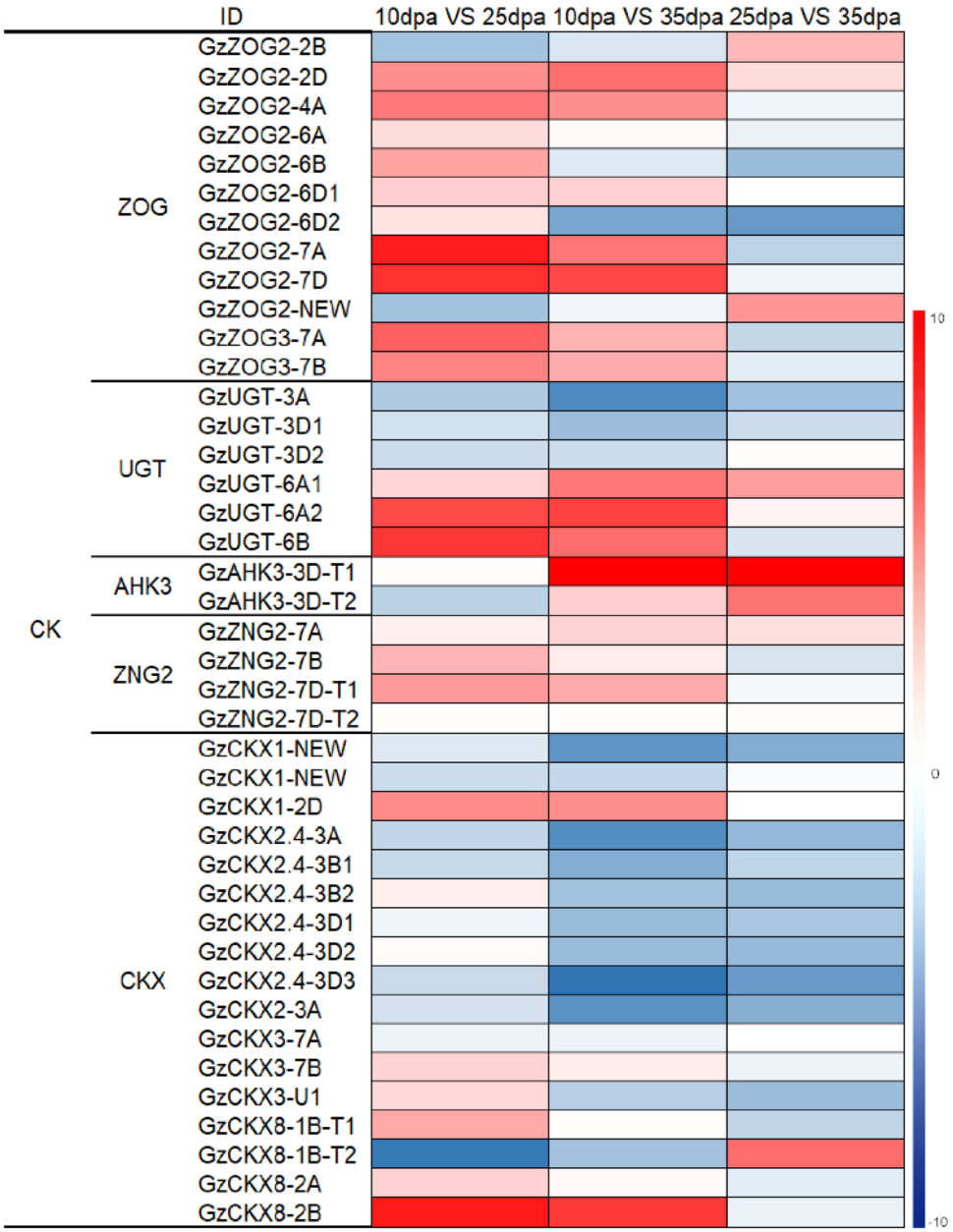


**Fig. 4** Heat map of cytokinin-pathway genes, including copies and alternatively spliced transcripts during anthocyanin accumulation in GZ1 grains. Different combinations of numbers and letters (7A, 7B, 7D, 1B, 1D, etc.) represent different chromosomal locations. "New" indicates that the chromosomal location is presently not clear. The same chromosome with different numbers represents corresponding copies of a gene located on that chromosome. Numbers after a capital "T" (T1, T2, T3, etc.) represent alternatively spliced transcripts of corresponding genes or copies

decreased from 25 to 35 dpa; and Gz*CKX8*-1B decreased from 10 to 25 dpa and then increased from 25 to 35 dpa. Our results demonstrated that different copies or alternative splicing transcripts showed different expression pattern, which may be responsible for different biological function.

## The qRT-PCR Validation of Auxin- and CK-Pathway Gene Expression Levels During Anthocyanin Accumulation in GZ1 Grains

To confirm the expression patterns of auxin- and CK-pathway genes related to anthocyanin biosynthesis in GZ1 grains, eight auxin- and CK-pathway genes, copies, or their alternatively spliced transcripts were selected for qRT-PCR validation. Among the former, Gz*IAA12*-5A (Fig. 5c) and Gz*5NG4*-7A1 (Fig. 5h) were upregulated during anthocyanin biosynthesis. Gz*ARF13*-7D (Fig. 5d) and Gz*AKR1*-7B2 (Fig. 5g) were downregulated. Gz*PIN1*-7B (Fig. 5a), Gz*LAX3*-1D (Fig. 5b), and Gz*ABP1*-5D (Fig. 5f) were significantly increased at 25 dpa and then reduced by 35 dpa compared to 10 dpa, in contrast to Gz*ARF17*-7A-T1 (Fig. 5e), which was significantly reduced at the 25 dpa and then significantly increased by 35 dpa. Among the latter, Gz*ZOG2*-2D (Fig. 6a) and Gz*AHK3*-3D-T1 (Fig. 6e) were upregulated during anthocyanin biosynthesis. Gz*UGT*-3D1 (Fig. 6d), Gz*CKX2*-3A (Fig. 6g), and Gz*CKX2.4*-3D3

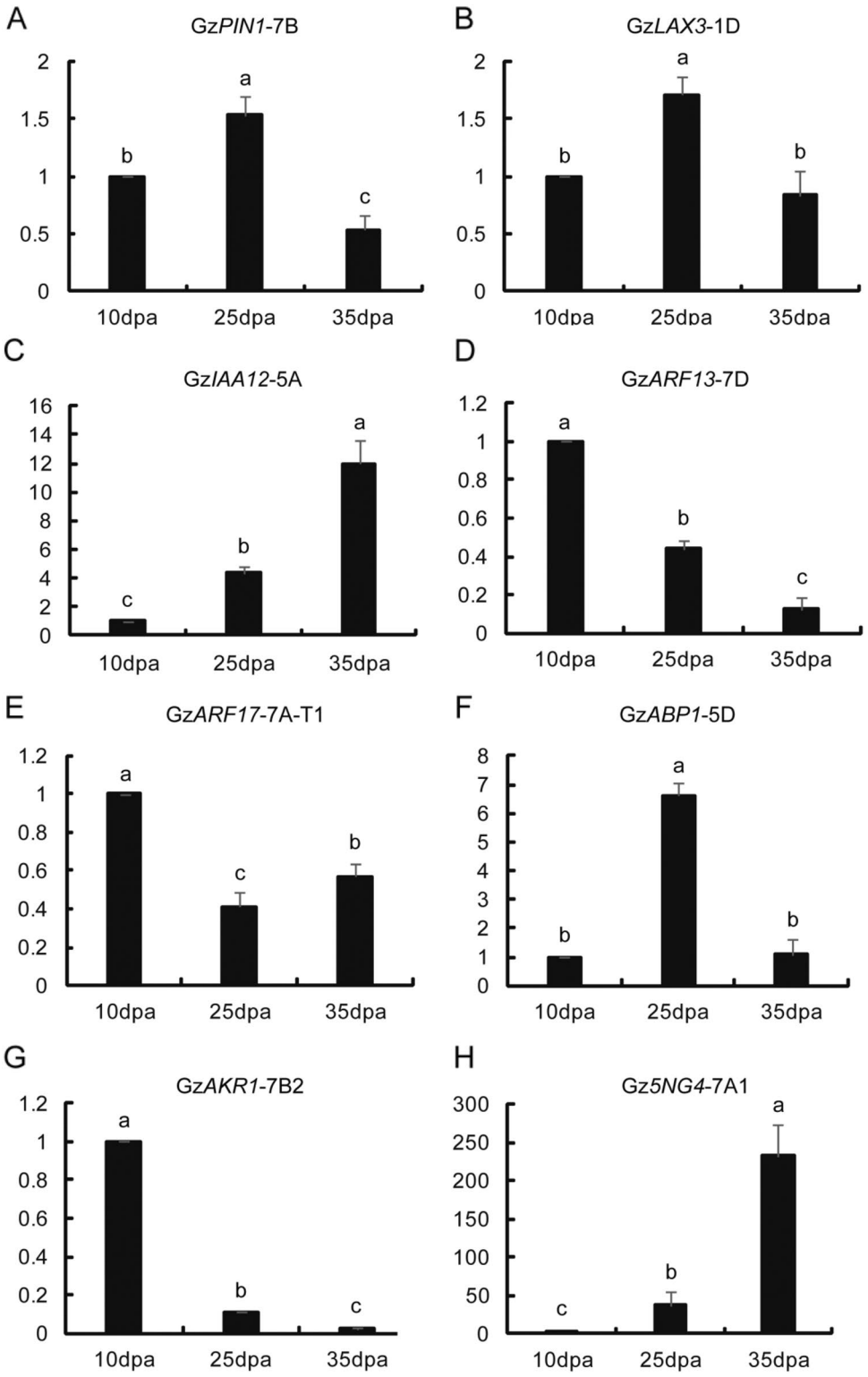


**Fig. 5** The qRT-PCR validation of auxin-pathway genes involved in anthocyanin biosynthesis in GZ1 grains. Each bar shows the mean ± SD of triplicate assays. A-H) the expression pattern of Gz*PIN1*-7B, Gz*LAX3*-1D, Gz*IAA12*-5A, Gz*ARF13*-7D, Gz*ARF17*-7A-T1, Gz*ABP1*-5D, Gz*AKR1*-7B2, and Gz*5NG4*-7A1 at different grain development stages 10dpa, 20dpa, and 35dpa, respectively. Different letters represent significant differences ($P < 0.05$)

(Fig. 6h) were downregulated. Gz*ZOG2*-7D (Fig. 6b) and Gz*ZOG3*-7A (Fig. 6c) were significantly increased at 25 dpa and then significantly reduced by 35 dpa compared to 10 dpa, while Gz*CKX1*-2D significantly increased and then slightly decreased.

## Dynamic Changes in the Auxin and CKs Contents During Anthocyanin Accumulation in GZ1 Grains

We determined the dynamic changes in the endogenous auxin and CK contents during anthocyanin accumulation

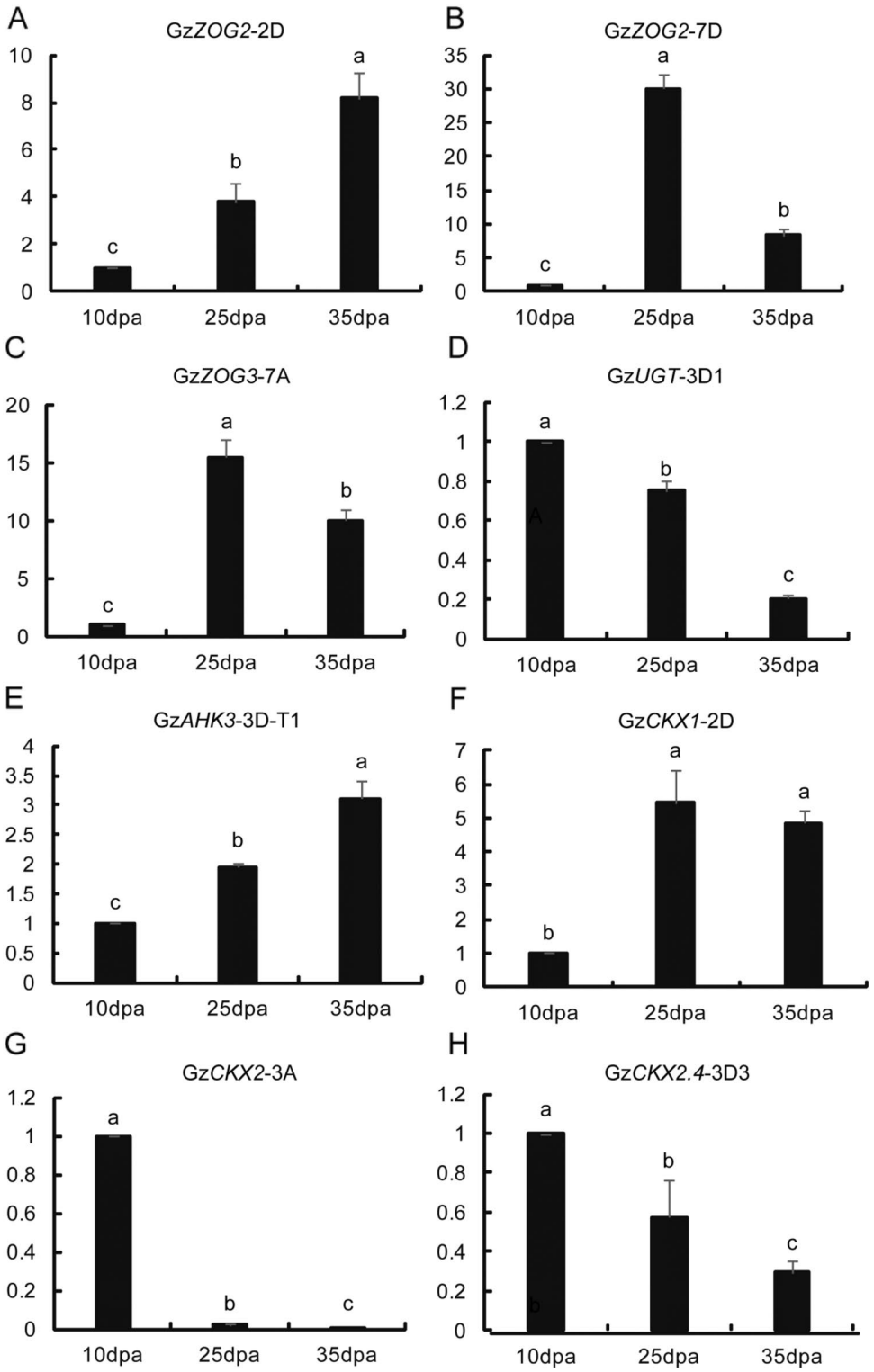


**Fig. 6** The qRT-PCR validation of cytokinin-pathway genes involved in anthocyanin biosynthesis in GZ1 grains. **a**–**h** the expression pattern of Gz*ZOG2*-2D, Gz*ZOG2*-7D, Gz*ZOG3*-7A, Gz*UGT*-3D1, Gz*AHK3*-3D-T1, Gz*CKX1*-2D, Gz*CKX2*-3A, and Gz*CKX2.4*-3D3 at different grain development stages 10dpa, 20dpa, and 35dpa, respectively. Each bar shows the mean ± SD of triplicate assays. Different letters represent significant differences ($P < 0.05$)

in GZ1 grains. The endogenous auxin (IAA) content significantly increased at 25 dpa and then decreased by 35 dpa compared to 10 dpa (Fig. 7a). The contents of five individual active CKs, iPR, cZ, czR, tZ, and tZR, were detected. During anthocyanin accumulation, the iPR and czR contents significantly decreased (Fig. 7b and d). The tZ contents at 25 dpa and 35 dpa, were significantly lower than the level at 10 dpa (Fig. 7e). In contrast to the IAA content, the cZ and tZR contents were significantly decreased at 25 dpa and then increased by 35 dpa

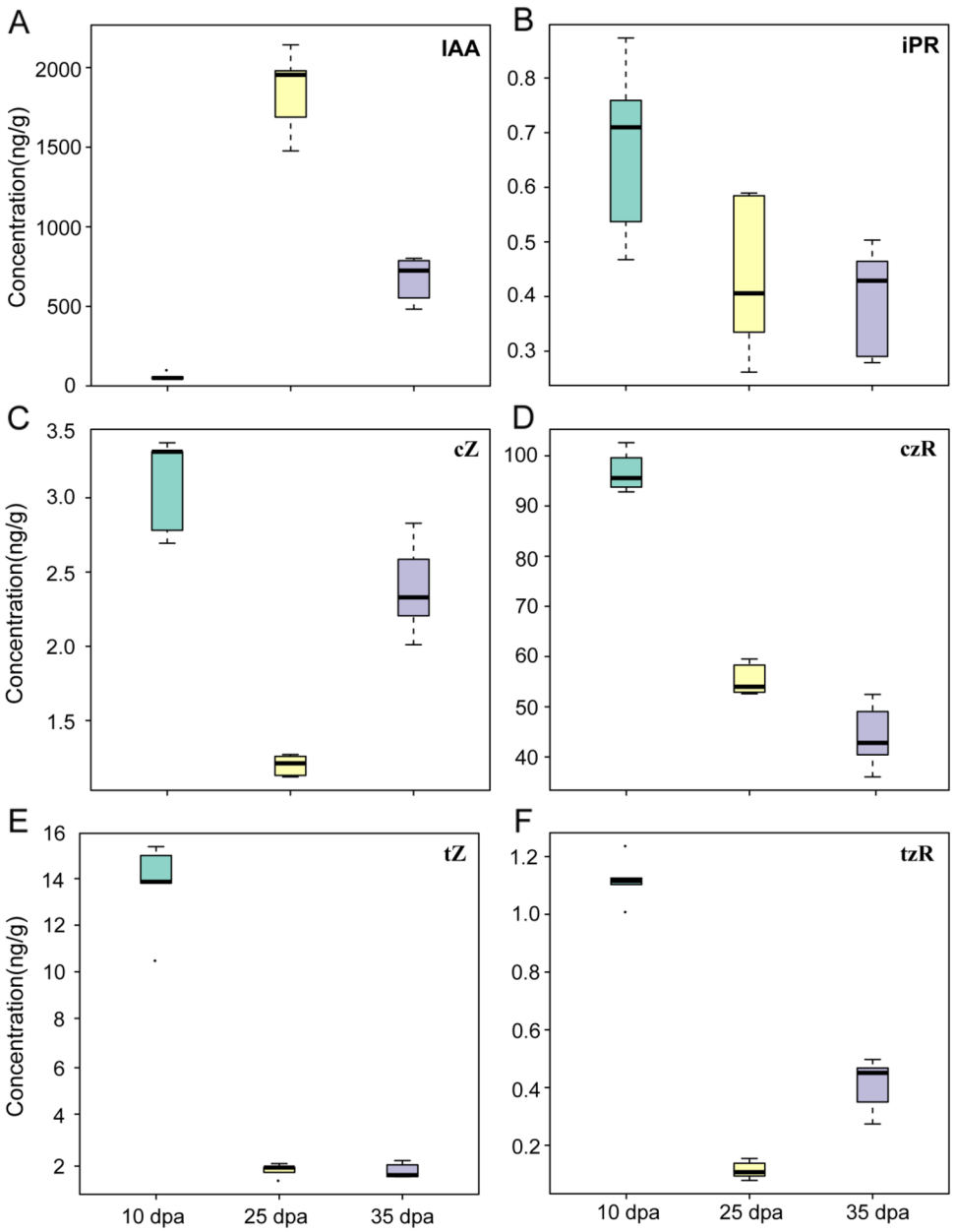


**Fig. 7** Auxin and cytokinin contents during anthocyanin accumulation in GZ1 grains. **a** Changes of IAA content during anthocyanin accumulation; **b–f** Changes of CKs (iPR, cZ, czR, tZ, and tzR, respectively) content during anthocyanin accumulation. Each bar shows the mean ± SD of three biological replicates

(Fig. 7c and f). In summary, the auxin and CKs may play antagonistic roles during anthocyanin accumulation in GZ1 grains.

### Antioxidant Enzyme Contents During Anthocyanin Accumulation in GZ1 Grains

Furthermore, we detected the contents of the antioxidant enzymes POD, CAT and SOD (Fig. 8). The POD and CAT contents were significantly increased at 25 dpa and then decreased by 35 dpa. However, the SOD content was significantly decreased at 25 dpa and then increased by 35 dpa.

## Discussion

Exogenous auxins and CKs regulate anthocyanin accumulation in plants (Liu et al. 2014; Park et al. 2016; Nguyen et al. 2015; Piazza et al. 2002; Ji et al. 2015; Jun et al. 2017). However, no information is available on the roles of auxin and CKs in the natural grain development of wheat. In this study, we explored the phenotypes of GZ1 grains at different development stages by observing and recording changes in the caryopsis size and anthocyanin content. By 20 dpa, GZ1 grains had basically reached their final size and the anthocyanin content started to gradually increase up to its maximum level (Fig. 1), which is in agreement with a previous study (Li et al. 2018).

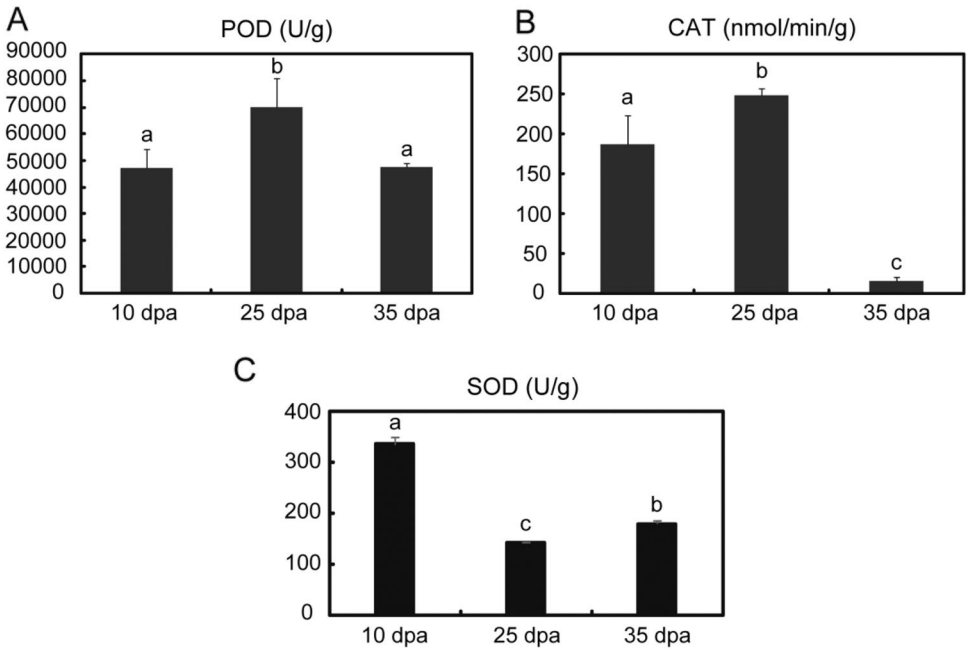


**Fig. 8** Contents of antioxidant enzymes during anthocyanin accumulation in GZ1 grains. Each bar shows the mean ± SD of three biological replicates. **a** Content of POD during anthocyanin accumulation; **b** Content of CAT during anthocyanin accumulation; **c** Content of SOD during anthocyanin accumulation. Different letters represent significant differences ($P < 0.05$)

Based on our previous transcriptome sequencing results, we determined that auxin-related genes (such as Gz*PIN1*, Gz*LAX3*, Gz*IAA12,* and Gz*ABP1*) and CKs-related genes (such as Gz*ZOG2*, Gz*UGT,* and Gz*CKX2*) may play important roles in anthocyanin accumulation during grain development (Figs. 3 and 4). Because of gene expression redundancy owing to polyploidy, the genes often contain multiple copies and alternative splice forms, which greatly increase transcript diversity (Himi and Noda 2004; Egawa et al. 2006; Yoo et al. 2014). Different copies or transcripts of genes, such as Gz*IAA16* and Gz*ZOG2*, did not exhibit exactly the same expression patterns, which demonstrated that these copies or transcripts may play different functions in the precise regulation of anthocyanin accumulation. The expression levels of auxin biosynthesis genes (such as *YUC*, *TAA,* and *TAR*) are low or even absent during the growth and ripening process (Yuan et al. 2019). Here, the *TAA* and *TAR* gene families were not detected, and only the Gz*YUCCA2* gene, at a low expression level, was detected during anthocyanin biosynthesis at different developmental periods, which indicated that the caryopsis is not the site of IAA biosynthesis in wheat (data not shown). In general, the expression patterns of Gz*IAA12*-5A, Gz*5NG4*-7A1, Gz*ARF13*-7D, Gz*ARF17*-7A-T1, Gz*ABP1*-5D, Gz*AKR1*-7B2, Gz*UGT*-3D1, Gz*CKX2*-3A, Gz*CKX2.4*-3D3, Gz*ZOG2*-7D, and Gz*ZOG3*-7A as assessed by qRT-PCR were consistent with our previous transcriptome sequencing results (Li et al. 2018). Furthermore, polar auxin carriers (Gz*PIN1* and Gz*LAX3*), auxin receptors (Gz*ABP* and Gz*ARP*) and signaling components (most of the Gz*ARF*s and Gz*AUX/IAA*s) at 25 dpa and 35 dpa showed significantly higher expression levels than at 10 dpa, having patterns that increased from 10 to 25 dpa and then decreased from 25 to 35 dpa (Figs. 3 and 5), which was consistent with our dynamic anthocyanin accumulation rate results (Fig. 1c) and the dynamic changes in the endogenous auxin content during anthocyanin accumulation in GZ1 grains (Fig. 7a). The high level of auxin at 25 dpa demonstrated that a rapid anthocyanin accumulation required a higher auxin content, which was in agreement with results in Tartary buckwheat (Park et al. 2016). However, our results were similar to those of Li et al. (2018) in which anthocyanin accumulation had normal levels of variation among different years owing to the environmental conditions (Liu et al. 2005; Knievel et al. 2009). CK homeostasis is precisely regulated owing to distinct developmental requirements. CK degradation genes (such as *CKX*) and inactivation genes (such as *UGT*) play important roles in maintaining CK homeostasis (Smehilova et al. 2016). Here, our results demonstrated that *GzCKX* (Gz*CKX1*, Gz*CKX2*, Gz*CKX2.4,* and Gz*CKX8*) and Gz*UGT* genes gradually decreased (Figs. 4 and 6), which means the enhanced degradation and/or inactivation of endogenous CK is gradually eliminated. The differential expression of Gz*CKX3* may be related to its diverse roles in CK homeostasis maintenance (Koellmer et al. 2014). Nguyen et al. confirmed that the repression of CK signaling leads to increased anthocyanin biosynthesis in *Arabidopsis* (Nguyen et al. 2016). Combined with the decreasing endogenous CK content (Fig. 7b–f), these results led us to propose that CK negatively regulates anthocyanin accumulation in natural GZ1 grain development. In addition, Gz*ZOG*s, Gz*ZNG*s, and Gz*AHK*s also participate in this process. Auxins and CKs interact during anthocyanin biosynthesis in plants (Ji et al. 2015; Teribia et al. 2016). Recently, a comparative transcriptome analysis of purple grain wheat

demonstrated that auxin- and CK-related genes participate in the light-promoted anthocyanin accumulation process (Wang et al. 2018). We determined that auxins and CKs may play antagonistic roles in anthocyanin accumulation by regulating related genes in purple wheat grain development.

Both anthocyanins and antioxidant proteins (such as POD, CAT, and SOD) can act as ROS-scavenging antioxidants to protect cells from stress by reducing the ROS level (Mittler et al. 2011; Nakabayashi et al. 2014; Lotkowska et al. 2015). Here, the antioxidant protein contents were detected and had different trends (Fig. 8). In particular, the dynamic changes in POD and CAT content were consistent with the dynamic change in the anthocyanin accumulation rate (Fig. 1c), which implied that ROS signaling participates in the regulation of anthocyanin accumulation. Thus, the coordinated promotion of auxin signaling and repression of CK signaling lead to increased anthocyanin biosynthesis during the natural grain development of purple wheat. Interestingly, different copies or transcripts of the same auxin- and CK-related genes showed diverse expression patterns. Thus, further research is required to elucidate this complex network underlying the auxin and CK signaling involved in anthocyanin accumulation.

**Acknowledgements** This project was supported by grants from the Guizhou Science and Technology Plan Project ([2019] 1073), the Guizhou Science and Technology Plan Project ([2020] 1Z018), the National Natural Science Foundation of China (31660390), and Construction Program of Biology First-class Discipline in Guizhou (GNYL [2017] 009). We thank International Science Editing (https://www.internationalscienceediting.com ) for editing this manuscript.

**Author Contributions** GY performed the experiments. MR and LL did the data collection. YP participated in experiments. RX designed the study. LL and ZW wrote the manuscript.

## Compliance with Ethical Standards

**Conflict of interest** The authors declare that they have no conflicts of interest.

## References

Bartl P, Albreht A, Skrt M, Tremlová B, Ošťádalová M, Šmejkal K, Vovk I, Ulrih NP (2015) Anthocyanins in purple and blue wheat grains and in resulting bread: quantity, composition, and thermal stability. J Agr Food Chem 66:514–519. https://doi.org/10.3109/09637486.2015.1056108

Brown DE, Aaron MR (2001) Flavonoids act as negative regulators of auxin transport in vivo in *Arabidopsis*. Plant Physiol 126:524–535. https://doi.org/10.1104/pp.126.2.524

Buer CS, Muday GK (2004) The transparent testa4 mutation prevents flavonoid synthesis and alters auxin transport and the response of *Arabidopsis* roots to gravity and light. Plant Cell 16:1191–1205. https://doi.org/10.1105/tpc.020313

Cavalcanti RN, Santos DT, Meireles MAA (2011) Non-thermal stabilization mechanisms of anthocyanins in model and food systems–an overview. Food Res Int 44:499–509. https://doi.org/10.1016/j.foodres.2010.12.007

Chen J, Mao L, Lu W, Ying T, Luo Z (2016) Transcriptome profiling of postharvest strawberry fruit in response to exogenous auxin and abscisic acid. Planta 243:183–197. https://doi.org/10.1007/s00425-015-2402-5

Chen W, Müller D, Richling E, Wink M (2013) Anthocyanin-rich purple wheat prolongs the life span of *Caenorhabditis elegans* probably by activating the DAF-16/FOXO transcription factor. J Agr Food Chem 61:3047–3053. https://doi.org/10.1021/jf3054643

Das PK, Shin DH, Choi SB, Yoo SD, Choi G, Park YI (2012) Cytokinins enhance sugar-induced anthocyanin biosynthesis in *Arabidopsis*. Mol Cells 34:93–101. https://doi.org/10.1007/s10059-012-0114-2

Egawa C, Kobayashi F, Ishibashi M, Nakamura T, Nakamura C, Takumi S (2006) Differential regulation of transcript accumulation and alternative splicing of a dreb2 homolog under abiotic stress conditions in common wheat. Genes Genet Syst 81:77–91. https://doi.org/10.1266/ggs.81.77

Guo JX, Wang SF, Yu XY (2018) Polyamines regulate strawberry fruit ripening by abscisic acid, auxin, and ethylene. Plant Physiol 177:339–351. https://doi.org/10.1104/pp.18.00245

Hammer DPE (1995) Induction of anthocyanin accumulation by cytokinins in *Arabidopsis thaliana*. Plant Physiol 108:47–57. https://doi.org/10.1104/pp.108.1.47

Himi E, Noda K (2004) Isolation and location of three homoelogous dihydroflavonol-t-reductase (DFR) genes of wheat and their tissue-dependent expression. J Exp Bot 55:365–375. https://doi.org/10.1111/j.1467-7717.2008.01046.x

Hirawan R, Diehl-Jones W, Beta T (2011) Comparative evaluation of the antioxidant potential of infant cereals produced from purple wheat and red rice grains and LC-MS analysis of their anthocyanins. J Agric Food Chem 59:12330–12341. https://doi.org/10.1021/jf202662a

Huang KL, Ma GJ, Zhang ML (2018) The ARF7 and ARF19 transcription factors positively regulate phosphate starvation response in *Arabidopsis* roots. Plant Physiol 178:413–427. https://doi.org/10.1104/pp.17.01713

Ji XH, Wang YT, Zhang R, Wu SJ, An MM, Li M (2015) Effect of auxin, cytokinin and nitrogen on anthocyanin biosynthesis in callus cultures of red-fleshed apple (*Malus sieversii f. niedzwetzkyana*). Plant Cell Tissue Org 120:325–337. https://doi.org/10.1007/s11240-014-0609-y

Jia H, Xie Z, Wang C, Shang GL, Qian N, Cui M (2017) Abscisic acid, sucrose, and auxin coordinately regulate berry ripening process of the Fujiminori grape. Funct Integr Genomic 17:441–457. https://doi.org/10.1007/s10142-017-0546-z

Jun BN, Song LB, Ling G, Min JQ, Lin BZ, Yuan WT (2017) Identification, classification, and transcription profiles of the B-type response regulator family in pear. PLoS ONE. https://doi.org/10.1371/journal.pone.0171523

Knievel DC, Abdel-Aal ESM, Rabalski I, Nakamura T, Hucl P (2009) Grain color development and the inheritance of high anthocyanin blue aleurone and purple pericarp in spring wheat (*Triticum aestivum* L.). J Cereal Sci 50:113–120. https://doi.org/10.1016/j.jcs.2009.03.007

Koellmer I, Novak O, Strand M (2014) Overexpression of the cytosolic cytokinin oxidase/dehydrogenase (CKX7) from *Arabidopsis* causes specific changes in root growth and xylem differentiation. Plant J 78:359–371. https://doi.org/10.1111/tpj.12477

Lazar G, Goodman HM (2006) MAX1, a regulator of the flavonoid pathway, controls vegetative axillary bud outgrowth in *Arabidopsis*. P Natl Acad Sci USA 103:472–476. https://doi.org/10.1073/pnas.0509463102

Li XL, Qian XK, Lǔ X, Wang XH, Ji N, Zhang MS, Ren MJ (2018) Upregulated structural and regulatory genes involved in

anthocyanin biosynthesis for coloration of purple grains during the middle and late grain-filling stages. Plant Physiol Biochem 130:235–247. https://doi.org/10.1016/j.plaphy.2018.07.011

Liu MS, Wang F, Dong YX, Zhang XS (2005) Expression analysis of dihydroflavonol 4-reductase genes involved in anthocyanin biosynthesis in purple grains of wheat. J Integr Plant Biol 47:1107–1114

Liu Q, Qiu Y, Beta T (2010) Comparison of antioxidant activities of different colored wheat grains and analysis of phenolic compounds. J Agric Food Chem 58:9235–9241. https://doi.org/10.1021/jf101700s

Liu Z, Shi MZ, Xie DY (2014) Regulation of anthocyanin biosynthesis in *Arabidopsis thaliana* red PAP1-D cells metabolically programmed by auxins. Planta 239:765–781. https://doi.org/10.1007/s00425-013-2011-0

Livak KJ, Schmittgen TD (2001) Analysis of relative gene expression data using real-time quantitative PCR and the $2^{-\Delta\Delta CT}$ method. Methods 25:402–408. https://doi.org/10.1006/meth.2001.1262

Lotkowska ME, Tohge T, Fernie AR, Xue GP, Balazadeh S, Mueller-Roeber B (2015) The *Arabidopsis* transcription factor MYB112 promotes anthocyanin formation during salinity and under high light stress. Plant Physiol 169:1862–1880. https://doi.org/10.1104/pp.15.00605

Ma D, Sun D, Wang C, Li Y, Guo T (2014) Expression of flavonoid biosynthesis genes and accumulation of flavonoid in wheat leaves in response to drought stress. Plant Physiol Biochem 80:60–66. https://doi.org/10.1016/j.plaphy.2014.03.024

Mittler R, Vanderauwera S, Suzuki N, Miller G, Tognetti VB, Vandepoele K, Gollery M, Shulaev V, Van BF (2011) Ros signaling: the new wave? Trends Plant Sci 16:300–309. https://doi.org/10.1016/j.tplants.2011.03.007

Murthy HN, Lee EJ, Paek KY (2014) Production of secondary metabolites from cell and organ cultures: strategies and approaches for biomass improvement and metabolite accumulation. Plant Cell Tissue Organ 118:1–16. https://doi.org/10.1007/s11240-014-0467-7

Nakabayashi R, Yonekura-Sakakibara K, Urano K, Suzuki M, Yamada Y, Nishizawa T (2014) Enhancement of oxidative and drought tolerance in *Arabidopsis* by overaccumulation of antioxidant flavonoids. Plant J 77:367–379. https://doi.org/10.1111/tpj.12388

Nguyen HN, Jeong CY, Kang GH (2015) MYBD employed by HY5 increases anthocyanin accumulation via repression of MYBL2 in *Arabidopsis*. Plant J 84:1192–1205. https://doi.org/10.1111/tpj.13077

Nguyen KH, Ha CV, Nishiyama R, Watanabe Y, Leyva-G MA, Fujita Y (2016) *Arabidopsis* type B cytokinin response regulators ARR1, ARR10, and ARR12 negatively regulate plant responses to drought. Proc Natl Acad Sci USA 113:3090–3095. https://doi.org/10.1073/pnas.1600399113

Olivares D, Contreras C, Muñoz V, Rivera S, González-Agüero M, Retamales J, Defilippi BG (2017) Relationship among color development, anthocyanin and pigment-related gene expression in 'Crimson Seedless' grapes treated with abscisic acid and sucrose. Plant Physiol Biochem 115:286–297. https://doi.org/10.1016/j.plaphy.2017.04.007

Park CH, AyeThwe A, Kim SJ (2016) Effect of auxins on anthocyanin accumulation in hairy root cultures of Tartary Buckwheat Cultivar Hokkai T10. Nat Prod Commun 11:1283–1286

Piazza P, Procissi A, Jenkins GI, Tonelli C (2002) Members of the c1/pl1 regulatory gene family mediate the response of maize aleurone and mesocotyl to different light qualities and cytokinins. Plant Physiol 128:1077–1086. https://doi.org/10.1104/pp.010799

Shao YL, Zhou HZ, Wu YR, Zhang H, Lin J, Jiang XY, He QJ, Zhu JS, Li Y, Yu H, Mao CZ (2019) OsSPL3, a SBP-domain protein, regulates crown root development in rice. Plant Cell. https://doi.org/10.1105/tpc.19.00038

Shi MZ, Xie DY (2011) Engineering of red cells of *Arabidopsis thaliana* and comparative genome-wide gene expression analysis of red cells versus wild-type cells. Planta 233:787–805. https://doi.org/10.1007/s00425-010-1335-2

Smehilova M, Dobruskova J, Novak O (2016) Cytokinin-specific glycosyltransferases possess different roles in cytokinin homeostasis maintenance. Front Plant Sci. https://doi.org/10.3389/fpls.2016.01264

Sytar O, Bośko P, Živčák M, Brestic M, Smetanska I (2018) Bioactive phytochemicals and antioxidant properties of the grains and sprouts of colored wheat genotypes. Molecules 23:2282. https://doi.org/10.3390/molecules23092282

Teribia N, Tijero V, Munne-Bosch S (2016) Linking hormonal profiles with variations in sugar and anthocyanin contents during the natural development and ripening of sweet cherries. New Biotechnol 33:824–833. https://doi.org/10.1016/j.nbt.2016.07.015

Wang F, Dong YX, Tang XZ, Tu TL, Zhao B, Sui N (2018) Comparative transcriptome analysis reveals effects of light on anthocyanin biosynthesis in purple grain of wheat. J Agric Food Chem 66:3465–3476. https://doi.org/10.1021/acs.jafc.7b05435

Yoo MJ, Liu X, Pires JC, Soltis PS, Soltis DE (2014) Nonadditive gene expression in polyploids. Annu Rev Genet 48:485–517. https://doi.org/10.1146/annurev-genet-120213-092159

Yuan HZ, Yu HM, Huang T (2019) The complexity of the Fragaria x ananassa (*Octoploid*) transcriptome by single-molecule long-read sequencing. Hortic Res. https://doi.org/10.1038/s41438-019-0126-6

Zeven AC (1991) Wheats with purple and blue grains: a review. Euphytica 56:243–258. https://doi.org/10.1007/BF00042371

Zhou LL, Zeng HN, Xie SDY (2008) Development of tobacco callus cultures over expressing *Arabidopsis* PAP1/MYB75 transcription factor and characterization of anthocyanin biosynthesis. Planta 229:37–51. https://doi.org/10.1007/s00425-008-0809-y

Zilić S, Serpen A, Akıllıoğlu G, Gökmen V, Vančetović J (2012) Phenolic compounds, carotenoids, anthocyanins and antioxidant capacity of colored maize (*Zea mays* L.) kernels. J Agric Food Chem 60:1224–1231. https://doi.org/10.1021/jf204367z